ISSN 0869-5911, Petrology, 2017, Vol. 25, No. 6, pp. 625–635. © Pleiades Publishing, Ltd., 2017.
Original Russian Text © S.Z. Smirnov, V.G. Thomas, V.S. Kamenetsky, O.A. Kozmenko, 2017, published in Petrologiya, 2017, Vol. 25, No. 6, pp. 646–658.

Hydrosilicate Liquids in the System Rare-Metal Granite–Na_2O–SiO_2–H_2O as Accumulators of Ore Components at High Pressure and Temperature

S. Z. Smirnov[a, b, *], V. G. Thomas[a], V. S. Kamenetsky[c, **], and O. A. Kozmenko[a]

[a] *Sobolev Institute of Geology and Mineralogy, Siberian Branch, Russian Academy of Sciences, Novosibirsk, 630090 Russia*
[b] *Tomsk State University, Tomsk, 634050 Russia*
[c] *ARC Center of Excellence in Ore Deposits, University of Tasmania, Hobart, Tasmania 7001, Australia*
**e-mail: ssmr@igm.nsc.ru*
***e-mail: Dima.Kamenetsky@utas.edu.an*

Received September 2, 2016; in final form, January 23, 2017

Abstract—Experimental investigations in the system rare-metal granite–Na_2O–SiO_2–H_2O with the addition of aqueous solutions containing Rb, Cs, Sn, W, Mo, and Zn at 600°C and 1.5 kbar showed that the typical elements of rare-metal granites (Li, Rb, Cs, Be, Nb, and Ta) are preferentially concentrated in hydrosilicate liquids coexisting with aqueous fluid. The same behavior is characteristic of Zn and Sn, the minerals of which are usually formed under hydrothermal conditions. In contrast, Mo and W are weakly extracted by hydrosilicate liquids and almost equally distributed between them and aqueous fluids. Liquids similar to those described in this paper are formed during the final stages of magmatic crystallization in granite and granite-pegmatite systems. The formation of hydrosilicate liquids in late magmatic and postmagmatic processes will be an important factor controlling the redistribution of metal components between residual magmatic melts, minerals, and aqueous fluids and, consequently, the mobility of these components in fluid-saturated magmatic systems enriched in rare metals.

DOI: 10.1134/S0869591117060054

INTRODUCTION

Experimental investigations in the system SiO_2–H_2O–AX, where AX is a salt component (A is an alkali ion, and X is a hydroxyl, carbonate, borate, or fluoride ion), at $T = 200$–800°C and $P = 1$–3 kbar showed that quartz and aqueous fluid (or aqueous solution at temperatures below the critical point) coexist with hydrosilicate liquids (HSL) consisting mainly of SiO_2 and H_2O in approximately equal molar proportions (Veksler, 2004; Smirnov et al., 2012).[1] Hydrosilicate liquids have relatively low viscosity (1–2 Pa s at 600°C according to our estimates) and slightly variable composition at a constant temperature over a wide range of the bulk composition of the system (Smirnov et al., 2005). A comparison of results reported by Mustart (1972), Kravchuk and Valyashko (1979), and Smirnov et al. (2005) suggests that the composition of HSL becomes richer in water and poorer in silica with decreasing temperature. This fact suggests that excess silica will precipitate from HSL as quartz at decreasing temperature. Such a scenario was supported by our observations (Smirnov et al., 2005, 2012) of the formation of well-faceted and skeletal quartz crystals up to several millimeters in size suspended in HSL. This allows us to consider HSL as a possible mineral-forming medium.

The addition of alumina to such systems does not prevent HSL formation; moreover, owing to an increase in the number of degrees of freedom, the composition of HSL becomes variable as a function of both temperature and the bulk composition of the system. With increasing bulk aluminum content, the major-element composition of HSL is shifted toward the nepheline syenite field (Thomas et al., 2014). The enrichment of HSL in alumina is accompanied by a decrease in their water content. These observations allow us to consider HSL as a transitional phase in a continuous transformation from silicate melt to aqueous fluid (Smirnov, 2015). In the silica–water and silicate–water systems, this is possible only at very high pressures (Kennedy et al., 1962; Schmidt et al., 2004; Kessel et al., 2005; Bureau and Keppler, 1999). The addition of B, F, and especially alkali metals to a water-saturated silica-rich aluminosilicate melt changes the topology of multiphase fields, and such a transformation becomes possible at temperatures of

[1] Hereafter, the term "fluid" refers to a substance in a supercritical state irrespective of its density (Valyashko, 1990).

Table 1. Composition of spodumene granite from the Alakhinskoe deposit

SiO_2	TiO_2	Al_2O_3	Fe_2O_3	CaO	MnO	K_2O	Na_2O	Li_2O	LOI	Total
74.51	0.018	15.57	0.087	0.14	0.024	2.43	5.69	1.25	0.52	100.26
Rb	Cs	Be	Nb	Ta	Zn	Mo	Sn		W	
933	149	124	64	154	66	0.27	2.5		0.95	

Major components (except Li) were analyzed by X-ray fluorescence; Li, by atomic absorption; and other trace metals, by ICP–MS. Major components are in wt %, and trace elements are in ppm.

~600°C and pressures of ~4 kbar (Sowerby and Keppler, 2002) close to the crystallization conditions of water-saturated rare-metal granite and pegmatite magmas (Smirnov, 2015).

A comparison of data on silicate liquid inclusions in minerals of granite pegmatites with experimental results shows, if not perfect coincidence, at least their significant overlapping in terms of major component contents: SiO_2, Al_2O_3, total alkali, and water (Thomas et al., 2014; Smirnov, 2015). In this relation, it is reasonable to extend the proposed mechanism of HSL formation through polycondensation in a SiO_2- and Al_2O_3-saturated alkaline aqueous fluid (Thomas et al., 2014) to the formation of natural HSL.

By analogy with experimental HSL, it can be assumed that natural HSL are ultradispersed media (Smirnov et al., 2005, 2012). During polycondensation, the extensive free surface of microscopic HSL droplets can adsorb metals dissolved in aqueous fluid. The considerable accumulation of Li, Cs, Be, Ta, Nb, W, and Sn in some mineral complexes of miarolitic pegmatites (Zagorsky and Peretyazhko, 1992; Zagorsky et al., 1999) could also be explained in such a case by the ultradispersed nature of the parental HSL.

Taking into account the above considerations, it is interesting to *explore experimentally the ability of HSL to concentrate various metals contributing to mineralization genetically related to the development of granite and granite pegmatite systems.* The goal of this study is to evaluate the distribution of ore components between coexisting crystal phases, HSL, and alkaline aqueous fluid. This work was begun by Smirnov et al. (2012), who studied Ta distribution.

EXPERIMENTAL AND ANALYTICAL METHODS

The problem was addressed in the system rare-metal granite–SiO_2–H_2O–Na_2O, in which the formation of HSL was previously observed (Thomas et al., 2014). Ore components were introduced as an aqueous solution containing NaOH, and in some cases their only source was the rare metal granite. In some experiments, NaF or NaCl was added as typical mineralizing components. The chemical analysis of experimental products revealed a very heterogeneous distribution of trace components in quenched HSL. Because of this, we conducted an experiment in a simpler system, SiO_2–H_2O–Na_2O–Ta, which we studied previously (Smirnov et al., 2012); it aimed at determining the spatial distribution of Ta in the column of HSL and the reasons of the nonuniform entrapment of this admixture.

Hydrothermal Experiments

Starting materials for experiments were prepared from distilled water; reagent-grade NaOH, NaCl, and NaF; a Ta metal plate (99.9% purity); and powder of spodumene granite from the Alakhinskoe deposit (Gornyi Altai) with a grain size of <0.25 mm. The granite composition (Table 1) corresponds to the modal mineral assemblage (wt %) of albite (48.14), microcline (14.35), spodumene (13.07), and quartz (23.69), with a total of 99.25. Silica was added as either synthetic quartz powder (grain size <0.25 mm) or a plate with dimensions of ~30 mm × ~5 mm × 1–2 mm sawn from a synthetic quartz crystal (one plate per run) normally to the *c* axis. The quartz plates were used as seeds for the entrapment of synthetic HSL inclusions owing to seed regeneration during the experiment. The compositions of initial charges are given in Table 2.

The experiments were performed in hermetically sealed gold capsules with a volume of ~10 mL. In the experiments with granite, a quartz plate was inserted vertically into the capsule, and the remaining free space was filled with intimately mixed starting materials. In the experiment in the SiO_2–Na_2O–H_2O–Ta system (Table 2, run 14), a Ta metal plate was placed at the bottom of the capsule and covered with quartz powder. The capsule with a solid charge was filled with aqueous solution (its compositions is given below), sealed by arc welding, and inserted into a Cr–Ni–Ti steel autoclave with a volume of ~220 mL. Half of the free vessel volume (autoclave volume minus capsule volume) was filled with distilled water, which provided a pressure of 1.5 kbar within the capsule at 600°C. The sealed autoclave was heated from room temperature to 600°C over 8 h and exposed at this temperature for 18 days. Temperature was controlled by two chromel–

Table 2. Starting charges (in g) loaded into capsules in experiments in the granite–SiO_2–Na_2O–H_2O and SiO_2–Na_2O–H_2O–Ta systems

Run	SiO_2	SiO_2*	Granite	NaF	NaCl	Ta	Solution 1	Solution 2
8		0.80	5.08				5.4	
9		1.32	5.11	0.053			5.3	
10		0.58	5.10		0.076		5.4	
11		1.91	5.11					5.2
12		0.87	5.11	0.054				5.4
13		0.79	5.11		0.075			5.4
14	3.00					0.041	5.3	

* The compositions of solutions 1 and 2 are presented in the text.
SiO_2 in the form of a quartz seed.

alumel thermocouples located at the bottom of the autoclave and in the obturator. The capsule was placed in a gradient-free zone (<3°C over the capsule length), which had to prevent the development of convection.

After annealing at 600°C for at least 18 days, the autoclave was quenched in water to ambient temperature, and the capsules were weighed to check for leakage. Aqueous solution was separated from solid products and collected immediately after the opening of the capsule. The amount of liquid products was calculated from the difference between the weights of the filled and empty capsule by subtracting the weight of dry solid products. The extracted liquid experimental products were acidified with HCl to prevent gel formation and precipitation of dissolved silica.

To evaluate the capacity of HSL to concentrate the selected rare metals and Zn in the system granite–Na_2O–SiO_2–H_2O, two series of experiments were carried out (Table 2). The first series (runs 8–10) was aimed at determining what metals and in what amounts are extracted by aqueous solution from granite and what metals partition into HSL. For these experiments, aqueous NaOH solution was prepared; it added 0.5 g of the alkali to the bulk composition (solution 1). In the second series (runs 11–13), the metals of interest were added to this solution (solution 2) in such amounts that the total NaOH content was the same as in runs 8–10.

Solution 2 was prepared in the following manner. Approximately 35 mg of Sn and Zn were dissolved separately in 5 mL HCl and precipitated as hydroxides, which were dissolved in 25 mL of aqueous NaOH solution (12 g/L) to produce sodium stannate and zincate. Then, the solutions were combined, and the resulting liquid was mixed with WO_3, MoO_3 (which are dissolved in alkaline aqueous solutions as sodium tungstates and molybdates), RbCl, and CsCl (40–53 mg for different metals). The total solution volume was brought to 65 mL. The prepared solution was stable under normal conditions. The resulting solution filling the experimental capsule contained 200–400 ppm of various metals. The amount of the added solution provided bulk contents of the metals of approximately 100 ppm. Similar to the previous experimental series, NaCl and NaF were added to determine the influence of mineralizers on the character of metal partitioning between HSL and aqueous fluid.

Analytical Methods

The experimental solutions were analyzed by atomic absorption for Li, Rb, K, and Cs and ICP–MS for other metals. The contents of F and Cl were determined spectrophotometrically by the Th-arsenazo III procedure (Jeffrey, 1970), and Na was analyzed by neutron activation using a Perkin Elmer 400 spectrometer.

The major component compositions of vitreous experimental phases were measured by EDS X-ray microanalysis in accordance with the principles discussed by (Thomas et al., 2014). The contents of Li and other metals added in the experiments were determined by the laser ablation inductively coupled plasma mass spectrometry (LA-ICP-MS). The analyses were made using an Element-2 Thermo Scientific spectrometer coupled with a UP-213 (New Wave) laser system. An area free of crystalline phases was selected for analysis, and the signal was collected by scanning with the laser beam over a profile or an area. Mass calibration was performed using the NIST 612 standard. The content of Al determined by electron microprobe analysis was used as internal standard. To check the accuracy, Na contents determined by LA-ICP-MS and electron microprobe analysis were compared. The consistency between the Na contents determined by the EDS and LA-ICP-MS techniques was on average ±20% relative. Water content was estimated from the analysis of oxygen by the EDS method. The amount of oxygen that could be assigned to water was calculated by subtracting the

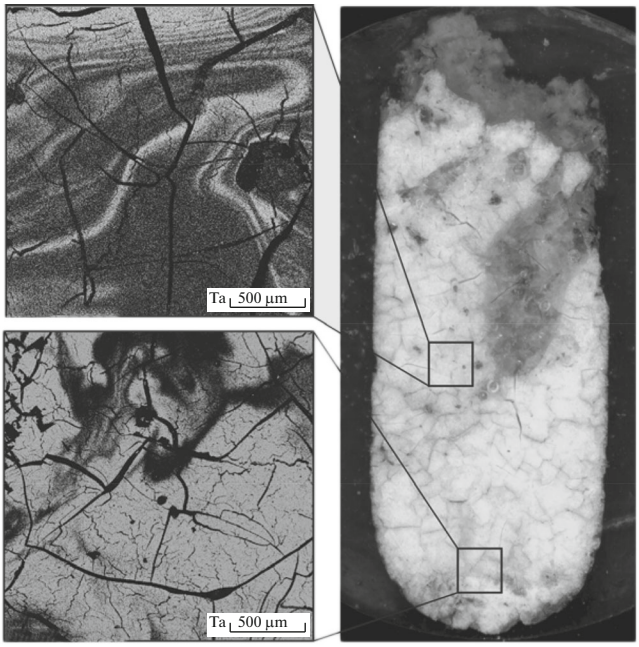

Fig. 1. Distribution of tantalum in the vitreous products of an experiment in the SiO_2–H_2O–Na_2O–Ta system (Table 2, run 14) determined by microprobe analysis. The right image shows the location of scanned areas in the column of solid experimental products, and maps of tantalum distribution in respective areas are shown on the left. Lighter and darker grey shades correspond to higher and lower tantalum contents, respectively. Black straight and broken lines are drying cracks appearing owing to sample dehydration in the microprobe vacuum chamber. Analyst D.V. Kuz'min.

mass of oxygen corresponding to the stoichiometry of all metal and silicon oxides from the total measured content of oxygen. The correctness of these estimates was checked by the analytical totals, which should approach 100%.

The distribution of Ta in the column of vitreous experimental products in the SiO_2–H_2O–Na_2O–Ta system was mapped with a JEOL JXA-8200 electron microprobe at the Max Planck Institute of Chemistry, Mainz, Germany. The analytical conditions were 20 kV accelerating voltage, 12 nA beam current, and 2 μm beam diameter. Mapping was conducted by measuring the intensity of the Ta-Lα line using a LiF wavelength dispersive spectrometer with a dwell time of 100 ms per spot. An area of approximately 2 mm^2 was mapped with a resolution of 1024 × 1024 pixels.

EXPERIMENTAL RESULTS

The quenched experimental products removed from the capsules consisted of a strongly alkaline (pH ≥ 14) aqueous solution and a compact column of solid phases. In the SiO_2–H_2O–Na_2O–Ta system (Table 2, run 14), the solid column consisted almost completely of a vitreous phase (Fig. 1), which was produced by HSL quenching. The upper boundary of the column is rough, because the HSL of this portion of the sample showed a rubber-like behavior upon cooling and was converted into powder after drying. The lowermost part of the column consisted of remnants of unreacted quartz grains without apparent evidence for regeneration cemented by a vitreous phase. Small crystals of a Na–Ta–Si-bearing phase, which was previously described by Smirnov et al. (2012), were observed at the very bottom of the capsule.

In the granite–SiO_2–H_2O–Na_2O system, clear glass occurs mainly on the surface of the column of solid products as a few millimeter-thick layer. It is underlain by a glassy layer containing remnants of the initial mixture (middle layer). The bottom portion of the column is composed of a porous aggregate of remnants of starting mixture cemented by a small amount of glass. In general, the structure of the column is similar to that described previously by Thomas et al. (2014). The solid columns from some experiments (runs 11 and 12) contain strongly resorbed relicts of the initial quartz blocks without evidence for regeneration, and the quartz blocks from other runs were completely dissolved. The spatial relations and thicknesses of the three layers are variable: the vitreous zone with remnants of the initial mixture may extend almost to the bottom of the column, and clear glass may occur as a small lens in the center of the column at the place of the quartz block (runs 12 and 13). In our opinion, such a character of phase distribution is related to the porosity of the starting mixture and its variable permeability to the formed HSL, which produced the vitreous phase upon quenching.

The composition of mineral phases, their quantitative relations, and structural characteristics of solid products from the experiments with solutions 1 and 2 in the granite–SiO_2–H_2O–Na_2O system are generally similar. Newly formed quartz crystals were not found. The crystalline phases are mainly feldspars, the composition of which corresponds to albite with up to 4% of the orthoclase component. Nepheline occurs in minor amounts and is extensively replaced by albite and sanidine.

Distribution of Ta in Vitreous Products from Experiments in the SiO_2–H_2O–Na_2O–Ta System

According to electron microprobe analysis, the average composition of glass from run 14 contains 65.3 wt % SiO_2, 16.6 wt % Na_2O, 0.68 wt % Ta_2O_5, and 0.5 wt % F. The results of mapping of Ta distribution in the vitreous phase are shown in Fig. 1. The Ta_2O_5 content varies considerably along the column and ranges from 0.05 to 1.6 wt % in the central part. Figure 1 illustrates the strongly heterogeneous distribution of the tantalum. This is especially conspicuous in the upper fragment of the column, where bands enriched in Ta alternate with portions of quenched HSL relatively poor

in Ta. The same is observed in the Ta-richer lower part: irregularly shaped embayments with relatively low Ta contents can be seen in the middle of the upper portion of this segment. Bands with higher Ta contents can be seen in these embayments.

In our opinion, these structures are not Liesegang rings (Efremov, 1971) resulting from the counter-diffusion of dissolved components through an ultradispersed medium and their subsequent interaction. Liesegang patterns must be perpendicular to the gradients of Ta, Si, Na, and H_2O concentrations, which is not the case (Fig. 1). The observed structures are more similar to the patterns formed during the slow laminar flow of two immiscible liquids. The portions of these liquids are not mixed and split into progressively thinner layers. Such flows patterns are formed in a liquid medium (HSL) with a viscosity of approximately 1–2 Pa s in a small capsule (~10 mm diameter) owing to gravity-driven convection at low temperature gradients (Gershuni and Zhukhovitskii, 1972).

In addition, the sharp boundaries between bands with higher and lower Ta contents are noteworthy. Smirnov et al. (2012) showed that HSL formation is accomplished almost completely within a few days. In our opinion, this means that there was no diffusive homogenization of Ta within ~10 days, which indicates insignificant Ta diffusion through the HSL.

Based on the model of Thomas et al. (2014), the described nonuniform Ta distribution in the HSL volume can be explained in the following way. A number of parallel and sequential processes occur during HSL formation:

(1) dissolution of metallic Ta at the bottom of the capsule in alkaline fluid;

(2) dissolution of quartz in alkaline fluid (lower part of the capsule);

(3) polymerization of dissolved silica with the formation and growth of micelles;

(4) sorption of dissolved Ta on the surface of growing micelles; and

(5) micelle adhesion and formation of macroscopic droplets of ultradispersed HSL enriched in Ta in the fluid volume and their gravitational settling to the capsule bottom or the surface of unreacted starting mixture.

As process 5 begins, the solid components reacting with the fluid are covered by a layer of newly formed HSL, and processes 1 and, then, 2 are terminated. If micelle formation and growth (process 3) continue, the fluid is rapidly depleted in Ta, because the partition coefficient of Ta (k(Ta) = C_{hsl}(Ta)/C_f(Ta), where C_{hsl}(Ta) and C_f(Ta) are the Ta contents in HSL and fluid, respectively) is much higher than one (Smirnov et al., 2012). As a result, the last portions of HSL will be strongly depleted in Ta. Two liquids are formed, rich and poor in Ta; they slide along each other without mixing (laminar flow) and form banded patterns (Fig. 1). A similar distribution of minor elements in HSL can be expected in the granite–SiO_2–H_2O–Na_2O system.

Composition of Vitreous Products in the Granite–SiO_2–H_2O–Na_2O System

The composition of glasses and solutions from the experiments are given in Tables 3 and 4, respectively. The rapid cooling (quenching) and alkaline pH (≥14) of the solutions after the experiments allow us to assume that the composition of solutions did not change during cooling as a result of the precipitation of components poorly soluble under normal conditions. In other words, we believe that the analyses given in Tables 3 and 4 correspond to the compositions of HSL and alkaline aqueous fluid coexisting at 600°C and 1.5 kbar.

It can be seen from Table 3 that the vitreous products of all experiments are not fundamentally different in major components (except for Li, Na, and F). As to Na and F, it is evident that NaF loaded in runs 9 and 12 was almost completely extracted by HSL, which resulted in proportional increases in Na and F contents. This inference is consistent with our previous data (Smirnov et al., 2012). In contrast, Cl partitions much less strongly into HSL, and the addition of NaCl to the system has therefore almost no effect on HSL composition. This implies the possibility of separation of two typical mineralizers, NaF and NaCl, between two coexisting phases of pegmatite and hydrothermal systems, HSL and aqueous fluid.

Noteworthy are considerable fluctuations of trace element contents between different points of glassy columns, significantly exceeding the analytical uncertainties (Table 3). Similarly to the behavior of Ta in the SiO_2–H_2O–Na_2O–Ta system, this can be explained by their nonuniform distribution in HSL (Fig. 1).

It would be instructive to use mass balance calculations for the evaluation of the redistribution of metals between starting solid phases, alkaline fluid, and HSL. The mass balances cannot be determined accurately even knowing the masses of the column of solid products and residual solution and the composition of the vitreous phase. The reason is that part of solution is retained in voids and pores (sometimes large) in the lower part of the column of solid products, and the newly formed vitreous phase cannot be separated from the remnants of starting materials. Nonetheless, approximate calculations can be made constraining the amount of the vitreous phase, M_{vf}, between upper and lower limits, $M' < M_{vf} < M''$. In order to determine M', it should be taken into account that quartz from the granite mixture was absent in the remnants of the starting mixture, and quartz seeds were not found in runs 8–10. Given the mass of the loaded granite (~5.1 g, Table 2, run 9) containing 24% quartz, the maximum mass of quartz seed completely dissolved during run 9 (~1.3 g), and H_2O content in the formed vitreous phase

Table 3. Average compositions of vitreous products of solidification of hydrosilicate liquids obtained in the granite–Na_2O–SiO_2–H_2O system at 600°C and 1.5 kbar with the addition of NaCl, NaF, and ore components

Component	$\pm\Delta_1$*, % abs	$\pm\Delta_2$**, % abs	Run					
			8	9	10	11	12	13
SiO_2	0.41	0.59	72.41	70.43	69.06	71.05	69.68	69.57
Al_2O_3	0.15	0.91	6.29	6.09	7.31	6.34	6.41	6.55
FeO			0.02	0	0	0	0	0
CaO	0.06	0.05	0.04	0.02	0.12	0.06	0.05	0.15
Na_2O	0.26	0.18	6.37	7.89	7.02	6.29	7.63	6.96
K_2O	0.11	0.18	2.66	2.37	3.37	2.57	2.58	2.74
Li_2O#	0.12	–	2.00	1.53	2.08	0.94	0.95	0.90
Cl	–	–	b.d.l.	b.d.l.	0.09	b.d.l.	b.d.l.	0.10
F	–	–	b.d.l.	0.55	b.d.l.	b.d.l.	0.56	b.d.l.
H_2O	–	0.05	11.10	11.15	11.10	11.10	11.05	11.10
Total			100.88	100.03	100.48	98.38	98.84	98.09
Be	31	67	124	198	138	198	95	180
Zn	51	**306**	43	26	46	428	504	490
Rb	251	**524**	892	770	822	1981	1518	1533
Nb	8	22	42	23	20	50	26	64
Mo	38	**110**	b.d.l.	b.d.l.	b.d.l.	190	220	167
Sn	158	**686**	b.d.l.	b.d.l.	b.d.l.	501	944	930
Cs	94	**290**	139	113	113	1006	736	717
Ta	10	24	59	46	23	49	41	86
W	70	**197**	b.d.l.	b.d.l.	b.d.l.	370	388	289

Li_2O was determined by secondary ion mass spectrometry in a single spot, and other trace elements were determined by LA-ICP-MS. Values obtained for runs 11–13 are shown in bold. A dash indicates that the value was not determined. Major components are in wt %, and trace elements are in ppm.
* Uncertainty of measurements. ** Amplitude of absolute deviations for various analysis spots.

Table 4. Compositions of aqueous solutions before and after experiments in the granite–Na_2O–SiO_2–H_2O system at 600°C and 1.5 kbar with the addition of NaCl, NaF, and ore components, ppm

Element	Starting compositions		After experiments with solution 1			After experiments with solution 2		
	Solution 1	Solution 2	8	9	10	11	12	13
Li	<0.1	<0.1	32	81	139	54	119	67
Na	57500	62100	940	1814	4930	1200	2640	1862
K	102	40	143	280	1931	260	588	780
Rb	–	530	8.7	15	135	28	51	74
Cs	<0.1	540	1.2	2	24	18	31	44
Be	<0.05	<0.05	<0.05	<0.05	<0.05	<0.05	<0.05	<0.05
Zn	<1	260	<1	<1	<1	<1	<1	<1
Nb	<0.02	<0.02	<0.02	<0.02	<0.02	<0.02	<0.02	<0.02
Mo	<0.02	500	1.8	1.7	2.3	321	312	166
Ta	<0.01	<0.01	<0.01	<0.01	<0.01	<0.01	<0.01	<0.01
Sn	1.5	410	<0.01	<0.01	<0.01	<0.01	<0.01	<0.01
W	0.9	500	2	1.3	1.7	140	157	146
Si	<5	3000	15	24	16	8	22	5
Al	<1	1000	<1	<1	<1	<1	<1	<1
F	–	–	–	1130	–	–	1050	–
Cl	–	–	–	–	4380	–	–	1850

A dash indicates that the element was not determined; 8–13 are run numbers.

(~11 wt %, Table 3), M' can be determined as (5.1 × 0.24 + 1.3) × 1.11 ≈ 2.7 g. A similar calculation for M'' assuming the complete dissolution of the starting material yields $M'' = (5.1 + 1.3) \times 1.11 \approx 7.1$ g.

Now let us calculate the amount of vitreous phase using the data of Tables 1–4 and assuming that all the minor elements added to the system were extracted into the vitreous phase except for those remaining in the solution after the experiment (Table 5). As can be seen in Table 5, only in some experiments, the amounts of vitreous phase calculated on the basis of Mo and Sn data appear to be underestimated (dark shaded cells in Table 5), which can be interpreted as resulting from the error of averaging of chemical analyses at strong variations in the contents of these trace elements. This error may result in a slight (no more than a factor of two) overestimation of the calculated partition coefficient, $k(E) = C_{hsl}(E)/C_f(E)$, where $C_{hsl}(E)$ and $C_f(E)$ are the contents of element E in the vitreous phase and residual solution after the experiment (Table 6).

The overestimation of the amount of vitreous phase (light shaded cells in Table 5) is interpreted as resulting from the incorporation of part of these elements in undissolved feldspar as either an isomorphic admixture or microinclusions of their own phases. Overestimations of the amounts of vitreous phase calculated by some of the elements occurred for all experiments, but they were not significant and can lead to a minor (no more than a factor of 3) underestimation of $k(E)$. It should be noted that the calculated coefficients are not strictly equivalent to the equilibrium partition coefficients (K_D) that are usually determined for coexisting homogeneous phases. They reflect the concentrating capacity of HSL coexisting with alkaline aqueous fluid in a steady state under the conditions of the absence of other phases concentrating the ore elements.

Based on the calculated partition coefficients (Table 6), the extraction capacity of HSL can be evaluated. It can be seen that the rare metals Li, Rb, Cs, Be, Nb, and Ta, which are mainly associated with rare-metal granites, are almost completely extracted by HSL from alkaline aqueous fluid. Zinc and tin, which are usually concentrated in natural hydrothermal assemblages, are also efficiently extracted by HSL. It is interesting that Mo and W, which tend to have an affinity with natural hydrothermal systems and related objects (greisens and skarns), are, in contrast, distributed equally between HSL and fluid (W) or partition preferentially into alkaline hydrothermal fluid (Mo).

The mineralizing components NaF and NaCl affect significantly only k(Li), k(Rb), and k(Cs). Their addition results in a several-fold decrease in these partition coefficients. However, they remain to be much higher than 1; i.e., these metals have a higher affinity for HSL. Moreover, the addition of Rb and Cs to the system as aqueous solution components results in a decrease in k(Li) (compare run 8 with run 11, run 9 with run 12, and run 10 with run 13). However, this decrease also does not change fundamentally the character of Li extraction by HSL.

Table 5. Results of the mass balance calculation of the amount of the vitreous phase (M_{vf}, g) using various trace elements (see text for explanation)

Component	Amount of vitreous phase (M_{vf}) in runs 8–13					
	8	9	10	11	12	13
Be	5.1	3.2	4.6	3.2	6.7	3.5
Zn	7.8	12.9	7.3	3.9	3.5	3.6
Rb	5.3	6.2	5.8	3.7	4.8	4.7
Nb	7.8	14.5	16.3	6.5	12.7	5.1
Mo	2.6	2.2	2.9	4.9	4.6	10.8
Sn	2.0	4.2	8.1	4.3	2.4	2.4
Cs	5.5	6.7	6.7	3.5	4.8	4.8
Ta	13.3	17.1	34.1	16.0	19.2	9.1
W	3.6	5.2	7.0	5.1	4.8	6.6
Li	3.2	4.2	2.7	6.8	7.2	7.1

Values in unshaded cells are calculated amounts of vitreous phase, M_{vf}, falling within the range 2.7 g < M_{vf} < 7.1 g, values in light gray cells are higher than the upper boundary, and values in dark gray cells are below the lower boundary.

Table 6. Partition coefficients, $k(E) = C_{hsl}(E)/C_f(E)$, of Li and trace elements in all experiments

Component (E)	$k(E) = C_{hsl}(E)/C_f(E)$ for runs 8–13					
	8	9	10	11	12	13
Be	>10	>10	>10	>10	>10	>10
Zn	>10	>10	>10	>10	>10	>10
Rb	103	51	6	71	30	21
Nb	>10	>10	>10	>10	>10	>10
Mo	0.3	0.4	0.2	0.6	0.7	1.0
Sn	>10	>10	>10	>10	>10	>10
Cs	116	57	5	56	24	16
Ta	>10	>10	>10	>10	>10	>10
W	0.7	0.7	0.4	2.6	2.5	2.0
Li	625	189	173	174	75	134

$C_{hsl}(E)$ and $C_f(E)$ are the contents of element E in the vitreous phase and residual solution after the experiment, respectively. Because of the closeness of the denominator to 0, *k(E)* could not be accurately calculated in some cases; taking into account the detection limits of the respective elements, $k(E)$ is undoubtedly >10, which is indicated in the table.

GEOLOGICAL APPLICATIONS OF THE EXPERIMENTAL RESULTS

Hydrosilicate liquids with the SiO_2/H_2O molar ratio close to one were obtained in the $SiO_2–H_2O$ system with the addition of Na_2O and Al_2O_3 (Mustart, 1972; Kravchuk, 1979), K_2O and Cs_2O (Morey and Fenner, 1917; Rumyantsev, 1999), Li_2O (Balitsky et al., 2000), NaF (Kotel'nikova and Kotel'nikov, 2002, 2004), NaF and H_3BO_3 (Peretyazhko et al., 2010), Na_2CO_3 (Butuzov and Bryatov, 1957; Kotel'nikova and Kotel'nikov, 2009; Wilkinson et al., 1996), and Na_2O and H_3BO_3 (Smirnov et al., 2005). These materials are transitional in their properties between silicate melts and aqueous solutions of silica or silicates. Hydrosilicate liquids could be produced by the normal evolution of water-saturated felsic melts enriched in B, F, and alkali metals at moderate to low pressures over a wide range of temperatures. Hydrosilicate liquids may be products of either the final stages of magma crystallization or interaction between silicate rocks and alkaline fluids derived from magmas. It should also be kept in mind that HSL formation was observed in experiments with compositions similar to natural granites and pegmatites at temperatures of 300–700°C and pressures of 1–2 kbar, i.e., below the water-saturated granite solidus. This implies that HSL can be formed at the stage of transition from magmatic to hydrothermal crystallization and during high-temperature postmagmatic processes.

The experimental results obtained in our study provide additional insight into the understanding of metal mobility in water–silicate systems and allow us to estimate the role of HSL in the redistribution of components. The physical properties of HSL allow their interpretation as colloidal systems (Smirnov et al., 2005, 2012; Thomas et al., 2014), which means that they are metastable and can only conditionally be considered in the phase equilibrium context. On the other hand, HSL can be formed in a wide range of *T–P–X* parameters relevant to geologic systems and exist for long periods of time (more than three months according to our unpublished observations).

The results of the previous work and experiments reported here suggest that colloidal HSL may be characteristic of heterogeneous chambers of granite pegmatite magmas enriched in H_2O, F, B, Li, and other rare metals (Peretyazhko et al., 2004a; Thomas and Davidson, 2012; Smirnov, 2015). Numerous investigations of fluid and melt inclusions in minerals from pegmatites of the aforementioned type have shown that their compositions are dominated by boric acid and alkali borates (Smirnov et al., 2000, 2003; Peretyazhko et al., 2000, 2004b; Thomas et al., 2003, 2008, 2012). Alkali bicarbonates may also be present (Thomas et al., 2011). This implies that such solutions have weakly alkaline pH values at high *T* and *P,* which is favorable for HSL formation (Smirnov et al., 2012; Thomas et al., 2014).

Based on the theoretical analysis of the behavior of fluid-saturated magmatic systems enriched in volatile and fluxing components and our experimental data, it can be concluded that there are two scenarios of HSL formation. They can be produced during the transformation of a fluid-saturated silicate melt into an aqueous fluid (Smirnov, 2015) or through interaction between an alkaline fluid and preexisting associations of silicate minerals (Thomas et al., 2014). These processes should be characteristic of the evolution of the fluid-saturated systems of miarolitic granite pegmatites with rare-metal mineralization and rare-metal Li–F granites.

The experimental results discussed in this paper indicate that HSL must play an important role in the concentration of elements associating with postmagmatic hydrothermal mineralization, which is usually connected with granites and granite pegmatites. In all cases, HSL concentrate preferentially alkali metals, including Li and Cs, compared with aqueous fluids. In contrast to normal silicate melts, Li is probably adsorbed by the colloidal solution of HSL and can be easily released from it at low temperatures (Thomas et al., 2014).

In addition to Li, HSL can efficiently concentrate practically all rare metals participating in ore formation. Our experiments showed that under the experimental conditions, the concentrations of Be, Zn, Nb, Sn, and Ta in HSL are tens or even hundreds of times greater than those in aqueous solutions. Moreover, HSL efficiently extract these metals from the rare-metal granite material and from aqueous solution. Tungsten and molybdenum show the lowest partition coefficients. This implies that the transport of W and Mo by aqueous fluids will be significant even in the presence of HSL. It was previously demonstrated that, in addition to ore metals, HSL can concentrate elements participating in mass transfer in hydrothermal systems, such as B (Smirnov et al., 2005) and F (Smirnov et al., 2012).

The obtained data are consistent with the results of experiments showing that HSL-like liquids can dissolve up to 15 wt % ZnS at 750°C and 1.2 kbar in the $Na_2Si_2O_5–H_2O$ system (Mustart, 1972) and up to 10.0–12.5 wt % MoS_2 at 650°C and 0.7 kbar in the $Na_2Si_2O_5–K_2Si_2O_5–H_2O$ system (Isuk and Carman, 1981).

The separated tiny HSL droplets can be dispersed in the intergranular space of the crystallizing magmatic body or be accumulated under favorable conditions. As inherently metastable phases, HSL can exchange components with aqueous fluid at decreasing temperature or decompose to form stable crystalline phases. In such a case, disseminated rare-metal mineralization (Li micas; Ta, Nb, and Sn oxides; etc.) will be formed in the intergranular space of granites or

granite pegmatites. However, when accumulated in sufficient amounts, HSL can from their own mineral complexes, which will be strongly different from the quartz–feldspar assemblages of granites or granite pegmatites. It can be suggested that such liquids must segregate to large bodies during the evolution of miarolitic granite pegmatites, because the magma-derived fluid phase is not removed from the system and takes part in all differentiation processes, up to the lowest temperatures (Peretyazhko, 2010).

Hydrosilicate liquids are readily formed in experiments under geologically realistic conditions. However, high-temperature mineral assemblages that could be reliably interpreted as products of the evolution of these liquids have not been established up to now. This can be explained by the peculiar nature of HSL. Based on the state of quench products and properties of HSL at high temperatures, which were investigated by Smirnov et al. (2005), they can be characterized as gels. A decrease in temperature and pressure must cause their structural transformations and coagulation, which will results in their decomposition. The compaction of coagulated gels (syneresis) induces the release of aqueous fluid enriched in those elements that were retained by adsorption. In our opinion, such elements are represented by Li in our experiments. Ageing or metasomatic alteration of the compacted HSL under the influence of aqueous solutions will result in the formation of new assemblages with high-grade ore mineralization within a pegmatite body at lower temperatures.

The formation of mineral aggregates at high temperatures and their subsequent alteration by pegmatite-derived hydrothermal solutions at decreasing temperature obscure evidence for the colloidal nature of initial HSL. Their relicts can be preserved only as inclusions in minerals isolated from the evolving system. Inclusions of natural silicate media with molar ratios of $SiO_2/H_2O \sim 1.6$ similar to the experimental products of HSL quenching ($SiO_2/H_2O = 1.1–1.4$) were found in minerals from miarolitic cavities in tourmaline-bearing granite pegmatites (Thomas et al., 2000, 2012; Smirnov et al., 2003; Peretyazhko et al., 2004b; Smirnov, 2015). At ambient temperature, they are composed of an aggregate of mica minerals and an aqueous boric acid solution. Upon heating up to 650°C at 3 kbar, the material of the inclusions was transformed to the association of immiscible aqueous fluid and HSL. During cooling, the HSL was transformed into a colorless transparent glass depleted in SiO_2 (57–68 wt %) relative to normal granite and strongly enriched in water (up to 15 wt %), F (3 wt %), and B_2O_3 (2.5 wt %). The total of alkalis may be as high as 13 wt %. A conspicuous feature of these glasses is that, in addition to K_2O and Na_2O, they are very rich in Li, Rb, Cs ($n \times 10^3$ to $n \times 10^4$ ppm), Ta, Nb, and Be, which makes them even more similar to the experimental HSL. These observations and the analysis of data on the mineralogy and petrography of various structural and compositional units of miarolitic granite pegmatites allow us to suggest that the evolution of natural pegmatitic HSL can produce mica and mica–albite assemblages with high-grade rare-metal mineralization surrounding the miarolitic cavities of granite pegmatites enriched in B, F, and rare metals (Zagorsky and Peretyazhko, 1992; Zagorsky et al., 1999; Zagorsky, 2012).

Owing to the low viscosity persisting to rather low temperatures of ~300°C, HSL can escape through fractures from the parental chamber over considerable distances to form mineralized veins. This is in line with the studies of other authors (Mustart, 1972; Wilkinson et al., 1996; Peretyazhko et al., 2004a; Kotel'nikova and Kotel'nikov, 2010, 2011a, 2011b), who argued that HSL-like liquids could play an important role in the transport of materials and mineral formation at the stage of transition from magmatic to hydrothermal crystallization in granitic and pegmatitic systems. It should be noted that the fluid released during syneresis can be enriched in ore components and is also an independent mineral- and ore-forming medium. It contributes to the formation of the latest mineral assemblages in pegmatites, granites, and contact aureoles of hydrothermal alteration.

Thus, it can be concluded that HSL formation during late magmatic and postmagmatic processes is an important factor controlling the redistribution of ore components between residual magmatic melts, minerals, and aqueous fluids and, as a consequence, the mobility of these components in fluid-saturated magmatic systems enriched in rare metals.

CONCLUSIONS

(1) It was found that hydrosilicate liquids (HSL), i.e., liquid media with SiO_2/H_2O molar ratios of ~1, can extract a number of ore components from alkaline aqueous fluids at a temperature of 600°C and a pressure of ~1.5 kbar. In particular, the typical elements of rare-metal granites Li, Rb, Cs, Be, Nb, and Ta are almost completely partitioned into HSL from initial aqueous fluid. The same is true for Zn and Sn, whose minerals crystallize mainly under hydrothermal conditions. In contrast, W and Mo are weakly extracted by HSL and are approximately equally distributed between aqueous fluid and HSL. Based on these observations, it was concluded that element fractionation between various mineral-forming media is possible already at the stage of HSL formation.

(2) Nonuniform uptake of trace elements by HSL was demonstrated by the example of Ta extraction by HSL in the $SiO_2–H_2O–Na_2O–Ta$ system. The reasons are, first, the absence of convective mixing in the HSL volume; second, the high partition coefficient of Ta between HSL and aqueous fluid (>10); third, the low diffusion rate of trace elements in HSL; and, fourth, the long time (several days) of HSL formation.

(3) It was shown that HSL formed in the granite–SiO_2–H_2O–Na_2O system promote the fractionation of both ore metals and mineralizing components. This can be exemplified by such typical mineralizers as NaF and NaCl: the former partitions preferentially into HSL, and the latter, into aqueous fluid.

(4) Liquids similar to HSL should be considered as potentially important media of ore metal transport and mineral formation at the stage of transition from magmatic to hydrothermal crystallization in granitic and pegmatitic systems.

ACKNOWLEDGMENTS

We are grateful to Doctor in Geology and Mineralogy, Prof. A.G. Vladimirov (Sobolev Institute of Geology and Mineralogy, Siberian Branch, Russian Academy of Sciences, Novosibirsk) for providing a sample of spodumene granite from the Alakhinskoe deposit for experiments. Hydrothermal experiments were carried out using facilities kindly made available by JV Tairus (Novosibirsk, Russia). We also thank A.G. Simakin (Institute of Experimental Mineralogy, Russian Academy of Sciences), whose comments helped to improve the manuscript. EDS and ICP-MS analyses were performed in the Center of Multielement and Isotopic Research of the IGM SB RAS.

This study was financially supported by the Russian Foundation for Basic Research, project no. 09-05-01153 and by the Program of Basic Research of the Siberian Branch of the Russian Academн of Sciences (project nos. VIII.66.1.2. and IX.125.1); CODES Initiative Grant P2.N1 "Phase and Chemical Composition of High-Temperature Hydrothermal Systems Undergoing Interaction between Silicate Rocks/Magmas and Aqueous Fluid," and the Australian Research Council Professorial Fellowship and Discovery Grant to V. Kamenetsky.

REFERENCES

Balitsky, V.S., Kurashige, M., Balitskaya, L.V., and Iwasaki, W., *Study of quartz solubility and "heavy" phase formation under industrial synthetic quartz growth conditions, Joint ISHR&ICSTR,* Kochi: Kochi University, 2000, pp. 318–321.

Bureau, H. and Keppler, H., Complete miscibility between silicate melts and hydrous fluids in the upper mantle: experimental evidence and geochemical implications, *Earth Planet. Sci. Lett.,* 1999, vol. 165, no. 2, pp. 187–196.

Butuzov, V.P. and Bryatov, L.V., Study of phase equilibria of the part of the H_2O–SiO_2–Na_2CO_3 system at high temperatures and pressures, *Kristallografiya,* 1957, vol. 204, no. 4, pp. 944–947.

Efremov, I.F., *Periodicheskie kolloidnye struktury* (Periodical Colloid Structures), Leningrad: Khimiya, 1971.

Gershuni, G.Z. and Zhukhovitskii, E.M., *Konvektivnaya ustoichivost' neszhimaemoi zhidkosti* (Convection Stability of Incompressible Liquid), Moscow: Nauka, 1972.

Isuk, E. and Carman, J., The system $Na_2Si_2O_5$–$K_2Si_2O_5$–MoS_2–H_2O with implications for molybdenum transport in silicate melts, *Econ. Geol.,* 1981, vol. 76, no. 8, pp. 2222–2235.

Jeffrey, P.G., *Chemical Methods of Rock Analysis,* Oxford: Pergamon Press, 1970.

Kennedy, G.C., Wasserburg, G.J., Heard, H.C., and Newton, R.C., The upper three-phase region in the system SiO_2–H_2O, *Am. J. Sci.,* 1962, vol. 260, pp. 501–521.

Kessel, R., Ulmer, P., Pettke, T., et al., The water–basalt system at 4 to 6 GPa: phase relations and second critical endpoint in K-free eclogite at 700 to 1400°C, *Earth Planet. Sci. Lett.,* 2005, vol. 237, pp. 873–892.

Kotel'nikova, Z.A. and Kotel'nikov, A.R., Synthetic NaF-bearing fluid inclusions, *Geochem. Int.,* 2002, vol. 40, no. 6, pp. 594–600.

Kotel'nikova, Z.A. and Kotel'nikov, A.R., NaF-bearing fluid inclusions in quartz synthesized at 450–500°C and P = 500–2000 bar, *Geochem. Int.* 2004, vol. 42, no. 8, pp. 794–798.

Kotel'nikova, Z.A. and Kotel'nikov, A.R., Liquid separation in the presence of vapor in synthetic fluid inclusions obtained from Na_2CO_3 solutions, *Dokl. Earth Sci.,* 2009, vol. 429, pp. 1533–1535.

Kotel'nikova, Z.A. and Kotel'nikov, A.R., Experimental study of heterogeneous fluid equilibria in silicate–salt–water systems, *Geol. Ore Deposits,* 2010, vol. 52, no. 2, pp. 171–185.

Kotel'nikova, Z.A. and Kotel'nikov, A.R., Unusual phase transformations in synthetic NaF-bearing fluid inclusions in quartz, *Dokl. Earth Sci.,* 2011a, vol. 439, no. 1, pp. 99–101.

Kotel'nikova, Z.A. and Kotel'nikov, A.R., The phase state of NaF-containing fluid at 700°C and 1, 2, and 3 kbar (from the results of study of synthetic fluid inclusions in quartz), *Russ. Geol. Geophys.,* 2011b, vol. 52, no. 11. pp. 1310–1318.

Kravchuk, K.G., Phase Equilibria in the SiO_2–Na_2O–H_2O System within a Wide Temperature and Pressure Range, *Extended Abstract of Cand. Sci. (Chem.) Dissertation,* Moscow: IONKh RAN, 1979.

Kravchuk, K.G. and Valyashko, V.M., *Phase Diagram of the SiO_2–$Na_2Si_2O_5$–H_2O System, Metody eksperimental'nogo issledovaniya gidrotermal'nykh ravnovesii* (Methods of Experimental Study of Hydrothermal Equilibria), Godovikov, A.A., Ed., Novosibirsk: Nauka, 1979, pp. 105–117.

Morey, G.W. and Fenner, C.N., The ternary system H_2O–K_2SiO_3–SiO_2, *J. Am. Chem. Soc.,* 1917, vol. 39, pp. 1173–1229.

Mustart, D.A., Phase Relations in the Peralkaline Portion of the System Na_2O–Al_2O_3–SiO_2–H_2O, *PhD Thesis,* Stanford: Stanford University, 1972.

Peretyazhko, I.S. Genesis of mineralized cavities (miaroles) in granite pegmatites and granites, *Petrology,* 2010, vol. 18, no. 2, pp. 183–208.

Peretyazhko, I.S., Prokof'ev, V.Yu., Zagorskii, V.E., and Smirnov, S.Z., Role of boric acids in the formation of pegmatite and hydrothermal minerals: petrologic consequences of sassolite (H_3BO_3) discovery in fluid inclusions, *Petrology,* 2000, vol. 8, no. 3, pp. 214–237.

Peretyazhko, I.S., Smirnov, S.Z., Thomas, V.G., and Zagorsky, V.Y., *Gels and melt-like gels in endogenous mineral formation, Metallogeny of the Pacific North West: Tectonics,*

Magmatism and Metallogeny of Active Continental Margins, Khanchuk A.I., Gonevchuk G.A., Mitrokhin A.N. et al., Eds., Vladivostok: Dal'nauka, 2004a, pp. 306–309.

Peretyazhko, I.S., Zagorsky, V.Y., Smirnov, S.Z., and Mikhailov, M.Y., Conditions of pocket formation in the Oktyabrskaya tourmaline-rich gem pegmatite (the Malkhan field, Central Transbaikalia, Russia), *Chem. Geol.,* 2004b, vol. 210, nos. 1–4, pp. 91–111.

Peretyazhko, I.S., Smirnov, S.Z., Kotel'nikov, A.R., and Kotel'nikova, Z.A., Role of boric acids in the formation of pegmatite and hydrothermal minerals: petrologic consequences of sassolite (H_3BO_3) discovery in fluid inclusions, *Russ. Geol. Geophys.,* 2010, vol. 51, no. 4, pp. 349–368.

Rumyantsev, V.N., Structure of crystal-forming environment and hydrothermal growth of quartz in NaOH aqueous solutions, *IV mezhdunarodnaya konferentsiya "Kristally: rost, svoistva, real'naya struktura i primenenie"* (4th International Conference on Crystals: Growth, Properties, Real Structure, and Application), Aleksandrov: VNIISIMS, TPU, 1999, vol. 1, pp. 16–38.

Schmidt, M.W., Vielzeuf, D., and Auzennau, E., Melting and dissolution of subducting crust at high pressures: the key role of white mica, *Earth Planet. Sci. Lett.,* 2004, vol. 228, pp. 65–84.

Smirnov, S.Z., The fluid regime of crystallization of water-saturated granitic and pegmatitic magmas: a physicochemical analysis, *Russ. Geol. Geophys.,* 2015, vol. 56, no. 9, pp. 1643–1663.

Smirnov, S.Z., Peretyazhko, I.S., Prokof'ev, V.Yu., et al., First find of sassolite (H_3BO_3) in fluid inclusions in minerals, *Geol. Geofiz.,* 2000, vol. 41, no. 2, pp. 194–206.

Smirnov, S.Z., Peretyazhko, I.S., Zagorskii, V.E., and Mikhailov, M.Yu., Inclusions of unusual late magmatic melts in quartz from the Oktyabr'skaya pegmatite vein, Malkhan Field (Central Transbaikal Region), *Dokl. Earth Sci.,* 2003, vol. 392, pp. 999–1003.

Smirnov, S.Z., Thomas, V.G., Demin, S.P., and Drebushchak, V.A., Experimental study of boron solubility and speciation in the Na_2O–B_2O_3–SiO_2–H_2O system, *Chem. Geol.,* 2005, vol. 223, nos. 1–3, pp. 16–34.

Smirnov, S.Z., Thomas, V.G., Kamenetsky, V.S., et al., Hydrosilicate liquids in the system Na_2O–SiO_2–H_2O with NaF, NaCl and Ta: evaluation of their role in ore and mineral formation at high *T* and *P, Petrology,* 2012, vol. 20, no. 3, pp. 271–285.

Sowerby, J.R. and Keppler, H., The effect of fluorine, boron and excess sodium on the critical curve in the albite–H_2O system, *Contrib. Mineral. Petrol.,* 2002, vol. 143, no. 1, pp. 32–37.

Thomas, R. and Davidson, P., Evidence of a water-rich silica gel state during the formation of a simple pegmatite, *Mineral. Mag.,* 2012, vol. 76, no. 7, pp. 2785–2801.

Thomas, R., Webster, J.D., and Heinrich, W., Melt inclusions in pegmatite quartz: complete miscibility between silicate melts and hydrous fluid at low pressure, *Contrib. Mineral. Petrol.,* 2000, vol. 139, pp. 394–401.

Thomas, R., Forster, H.J., and Heinrich, W., The behaviour of boron in a peraluminous granite-pegmatite system and associated hydrothermal solutions: a melt and fluid-inclusion study, *Contrib. Mineral. Petrol.,* 2003, vol. 144, no. 4, pp. 457–472.

Thomas, R., Davidson, P., and Hahn, A., Ramanite-(Cs) and ramanite-(Rb): new cesium and rubidium pentaborate tetrahydrate minerals identified with Raman spectroscopy, *Am. Mineral.,* 2008, vol. 93, no. 7, pp. 1034–1042.

Thomas, R., Davidson, P., and Schmidt, C., Extreme alkali bicarbonate- and carbonate-rich fluid inclusions in granite pegmatite from the Precambrian Ronne granite, Bornholm Island, Denmark, *Contrib. Mineral. Petrol.,* 2011, vol. 161, no. 2, pp. 315–329.

Thomas, R., Davidson, P., and Badanina, E.V., Water- and boron-rich melt inclusions on quartz from the Malkhan pegmatite, Transbaikalia, Russia, *Minerals,* 2012, vol. 2, pp. 435–458.

Thomas V.G., Smirnov S.Z., Koz'menko O.A., et al., Formation and properties of hydrosilicate liquids in the systems Na_2O–Al_2O_3–SiO_2–H_2O and granite–Na_2O–SiO_2–H_2O at 600°C and 1.5 kbar, *Petrology,* 2014, vol. 22, no. 3, pp. 327–344.

Valyashko, V.M., *Fazovye ravnovesiya i svoistva gidrotermal'nykh system* (Phase Equilirbia and Properties of Hydrothermal Systems) Moscow: Nauka, 1990.

Veksler, I.V., Liquid immiscibility and its role at the magmatic–hydrothermal transition: a summary of experimental studies, *Chem. Geol.,* 2004, vol. 210, nos. 1–4, pp. 7–31.

Wilkinson, J.J., Nolan, J., and Rankin, A.H., Silicothermal fluid: a novel medium for mass transport in the lithosphere, *Geology,* 1996, vol. 24, no. 12, pp. 1059–1062.

Zagorsky, V.E., Mineralogy of pockets of the Malkhan tourmaline deposit (Transbaikalia): feldspars of the Sosedka Vein, *Russ. Geol. Geophys.,* 2012, vol. 53, no. 6, pp. 522–534.

Zagorsky, V.E. and Peretyazhko, I.S., *Pegmatity s samotsvetami Tsentral'nogo Zabaikal'ya* (Pegmatites with Semiprecious Stones of Central Transbaikalia), Novosibirsk: Nauka, 1992.

Zagorsky, V.E., Peretyazhko, I.S., and Shmakin, B.M., *Granitnye pegmatity* (Granite Pegmatites), Novosibirsk: Nauka, 1999.

Translated by A. Girnis